

A GENERALIZED DIFFUSION TENSOR FOR FULLY ANISOTROPIC DIFFUSION OF ENERGETIC PARTICLES IN THE HELIOSPHERIC MAGNETIC FIELD

F. EFFENBERGER¹, H. FICHTNER¹, K. SCHERER¹, S. BARRA¹, J. KLEIMANN¹, AND R. D. STRAUSS²

¹Institut für Theoretische Physik IV, Ruhr-Universität Bochum, 44780 Bochum, Germany; fe@tp4.rub.de

²Centre for Space Research, North-West University, 2520 Potchefstroom, South Africa

Received 2011 December 22; accepted 2012 February 28; published 2012 April 20

ABSTRACT

The spatial diffusion of cosmic rays in turbulent magnetic fields can, in the most general case, be fully anisotropic, i.e., one has to distinguish three diffusion axes in a local, field-aligned frame. We reexamine the transformation for the diffusion tensor from this local to a global frame, in which the Parker transport equation for energetic particles is usually formulated and solved. Particularly, we generalize the transformation formulae to allow for an explicit choice of two principal local perpendicular diffusion axes. This generalization includes the “traditional” diffusion tensor in the special case of isotropic perpendicular diffusion. For the local frame, we describe the motivation for the choice of the Frenet–Serret trihedron, which is related to the intrinsic magnetic field geometry. We directly compare the old and the new tensor elements for two heliospheric magnetic field configurations, namely the hybrid Fisk and Parker fields. Subsequently, we examine the significance of the different formulations for the diffusion tensor in a standard three-dimensional model for the modulation of galactic protons. For this, we utilize a numerical code to evaluate a system of stochastic differential equations equivalent to the Parker transport equation and present the resulting modulated spectra. The computed differential fluxes based on the new tensor formulation deviate from those obtained with the “traditional” one (only valid for isotropic perpendicular diffusion) by up to 60% for energies below a few hundred MeV depending on heliocentric distance.

Key words: cosmic rays – diffusion – Sun: heliosphere

Online-only material: color figures

1. INTRODUCTION AND MOTIVATION

The most important transport process for energetic charged particles in the heliosphere is their spatial diffusion as a consequence of their interaction with the turbulent heliospheric magnetic field (HMF). While rarely used in models of galactic transport, the concept of *anisotropic diffusion* is well established (see, e.g., Burger et al. 2000; Schlickeiser 2002; Shalchi 2009) for models of heliospheric cosmic ray (CR) modulation. In most studies the anisotropy refers to a difference in the diffusion coefficient parallel (κ_{\parallel}) and perpendicular (κ_{\perp}) to the magnetic field, and the perpendicular diffusion is treated as being isotropic.

Although the notion of fully anisotropic diffusion is not new—see an early study by Jokipii (1973) considering for the first time *anisotropic perpendicular diffusion*, i.e., $\kappa_{\perp 1} \neq \kappa_{\perp 2}$ —it was not before the measurements made with the *Ulysses* spacecraft that this concept had to be used to explain the high-latitude observations of CRs; see, e.g., Jokipii et al. (1995), Potgieter et al. (1997), and Ferreira et al. (2001). These studies remained largely phenomenological and did not attempt a rigorous investigation of anisotropic perpendicular diffusion.

More recently, in the context of studies of the transport of solar energetic particles in the heliospheric Parker field, Tautz et al. (2011) and Kelly et al. (2012) have determined the elements of the diffusion tensor from test particle simulations in a local, field-aligned frame. While the former authors find no conclusive result, the latter authors clearly demonstrated that the scattering in the inhomogeneous Parker field can indeed induce anisotropic perpendicular diffusion.

Given this phenomenological and simulation-based evidence, it is important to determine the principal directions of perpendicular diffusion in the field-aligned local frame, because the transformation of the diffusion tensor from a correspondingly

oriented local coordinate system into a global coordinate system determines the exact form of the tensor elements in the latter, in which the transport equation is usually solved. This is of particular importance in the case of symmetry-free magnetic fields, like the so-called Fisk field (Fisk 1996). The latter is—although in a weaker manner than originally suspected (Lionello et al. 2006; Sternal et al. 2011)—still a valid generalization of the Parker field and takes into account a non-vanishing latitudinal field component.

While it has been recognized that the use of the Fisk field in models of the heliospheric modulation of CRs requires a re-derivation of the diffusion tensor (Kobylinski 2001; Alania 2002; Burger et al. 2008), the formulae given in these papers differ from each other and are either valid only for the case of isotropic perpendicular diffusion (the former two papers) or for a specific orientation of the local coordinate system (the latter paper). Consequently, there are two open issues, namely (1) to determine which of these formulae are correct (see also Appendix A) and (2) to generalize these results to the case of anisotropic perpendicular diffusion. With the present paper we address both issues by deriving general formulae for the transformation of a fully anisotropic diffusion tensor. In addition to establishing the appropriate description, we apply the new generalized formulae to a standard modulation problem in order to demonstrate the physical significance of the approach.

2. GENERAL CONSIDERATIONS

Anisotropic perpendicular transport can, in principle, result (1) from an inhomogeneous (asymmetric) magnetic background field or (2) from turbulence that is intrinsically non-axisymmetric with respect to the (homogeneous) local magnetic field direction (e.g., Weinhorst et al. 2008). While the

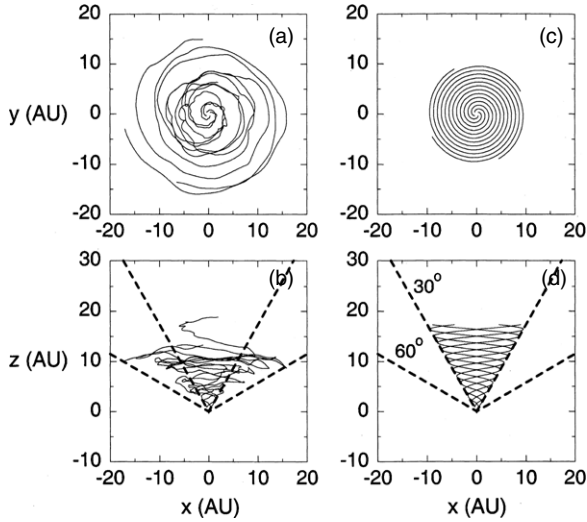


Figure 1. Undisturbed (right) heliospheric magnetic field (projected into the equatorial (top) and a meridional plane (bottom)) according to Parker (1958) and its structure when field line random walk is included (left), taken from Jokipii (2001).

latter case has been discussed in the context of energetic particle transport (Ruffolo et al. 2008) partly motivated by the observed ratios of the power in the microscale magnetic field fluctuations parallel and perpendicular to the background field: $\delta B_{\perp 1}^2 : \delta B_{\perp 2}^2 : \delta B_{\parallel}^2 = 5 : 4 : 1$ (where $\delta \vec{B}_{\perp 1}$ is aligned to the latitudinal unit vector and the normalized $\delta \vec{B}_{\perp 2}$ completes the local trihedron, see Belcher & Davis 1971; Horbury et al. 1995), recent analyses indicate that the perpendicular fluctuations are probably axisymmetric (Turner et al. 2011; Wicks et al. 2012). Therefore, we consider the first case of an inhomogeneous magnetic background field to be more likely to cause fully anisotropic diffusion.

If the random walk of field lines due to turbulence is significantly contributing to the perpendicular particle transport, one generally has to expect the latter to be anisotropic. This can be illustrated already for the simple case that the HMF is represented by the Parker spiral (see Figure 1). Due to the field geometry the field line wandering is not isotropic, neither in radial direction nor in heliographic latitude, resulting in a field line diffusion coefficient depending on both (Webb et al. 2009).

As soon as anisotropic perpendicular diffusion occurs, it is necessary to determine the principal axes of the diffusion tensor in a local field-aligned frame (\hat{k}_L), because their orientation determines the tensor elements in the global frame (\hat{k}) after a corresponding transformation given by

$$\hat{k} = A \hat{k}_L A^T \quad (1)$$

with

$$\hat{k}_L = \begin{pmatrix} \kappa_{\perp 1} & \kappa_A & 0 \\ -\kappa_A & \kappa_{\perp 2} & 0 \\ 0 & 0 & \kappa_{\parallel} \end{pmatrix} \quad (2)$$

where, in general, κ_A denotes the drift coefficient, induced by a non-axisymmetric turbulence and by inhomogeneous magnetic fields. The latter drifts can always be described by a drift velocity \vec{v}_d in the transport equation (Tautz & Shalchi 2012; Burger et al. 2008) and are therefore not considered in the following. In Equation (1), analogous to the Euler angle transformation known from classical mechanics, the matrix $A = R_3 R_2 R_1$ describes

three consecutive rotations R_i with $A^{-1} = A^T$. These rotations are defined by the relative orientation of the local and the global coordinate system with respect to each other.

Due to the latitudinal structuring of the solar wind and, in turn, of the Parker spiral having a vanishing B_{θ} -component, one may argue that in that case the latitudinal direction remains a preferred one so that the local coordinate system could always be defined by the unit vectors \vec{t} (along the field), \vec{e}_{θ} (from a spherical polar coordinate system) and $\vec{e}_{\theta} \times \vec{t}$. This, however, can obviously not be the case for symmetry-free fields like the Fisk field (Fisk 1996).

In general, the local trihedron will consist of a unit vector \vec{t} tangential to the magnetic field and two orthogonal ones, \vec{u} and \vec{v} , defining the remaining principal axes. With this notation the transformation (1) reads, for an arbitrary choice of this local trihedron:

$$\kappa_{11} = \kappa_{\perp 1} u_1^2 + \kappa_{\perp 2} v_1^2 + \kappa_{\parallel} t_1^2 \quad (3)$$

$$\kappa_{12} = \kappa_{\perp 1} u_1 u_2 + \kappa_{\perp 2} v_1 v_2 + \kappa_{\parallel} t_1 t_2 + \kappa_A (u_1 v_2 - u_2 v_1) \quad (4)$$

$$\kappa_{13} = \kappa_{\perp 1} u_1 u_3 + \kappa_{\perp 2} v_1 v_3 + \kappa_{\parallel} t_1 t_3 + \kappa_A (u_1 v_3 - u_3 v_1) \quad (5)$$

$$\kappa_{21} = \kappa_{\perp 1} u_1 u_2 + \kappa_{\perp 2} v_1 v_2 + \kappa_{\parallel} t_1 t_2 - \kappa_A (u_1 v_2 - u_2 v_1) \quad (6)$$

$$\kappa_{22} = \kappa_{\perp 1} u_2^2 + \kappa_{\perp 2} v_2^2 + \kappa_{\parallel} t_2^2 \quad (7)$$

$$\kappa_{23} = \kappa_{\perp 1} u_2 u_3 + \kappa_{\perp 2} v_2 v_3 + \kappa_{\parallel} t_2 t_3 + \kappa_A (u_2 v_3 - u_3 v_2) \quad (8)$$

$$\kappa_{31} = \kappa_{\perp 1} u_1 u_3 + \kappa_{\perp 2} v_1 v_3 + \kappa_{\parallel} t_1 t_3 - \kappa_A (u_1 v_3 - u_3 v_1) \quad (9)$$

$$\kappa_{32} = \kappa_{\perp 1} u_2 u_3 + \kappa_{\perp 2} v_2 v_3 + \kappa_{\parallel} t_2 t_3 - \kappa_A (u_2 v_3 - u_3 v_2) \quad (10)$$

$$\kappa_{33} = \kappa_{\perp 1} u_3^2 + \kappa_{\perp 2} v_3^2 + \kappa_{\parallel} t_3^2, \quad (11)$$

where the components of \vec{t} , \vec{u} , and \vec{v} are determined in the global coordinate system. Consequently, the task is to determine the unit vectors \vec{t} , \vec{u} , and \vec{v} for an arbitrary, symmetry-free magnetic field.

Given that the perpendicular fluctuations are probably axisymmetric (Turner et al. 2011; Wicks et al. 2012) as discussed above, we assume $\kappa_A = 0$ in the following.

With this explicit formulation of the tensor elements we can already address issue (1) defined in Section 1. For the case that the perpendicular diffusion is isotropic, i.e., $\kappa_{\perp 1} = \kappa_{\perp 2}$, the formulae given by Burger et al. (2008), see Appendix A, are identical to Equations (3)–(11), so that their correction of the results found by Kobylinski (2001) and Alania (2002) and, in turn, their subsequent analysis are validated. We emphasize, however, that neither of these formulations (involving only two rotation angles) allow the explicit definition of the perpendicular diffusion axes, which are necessary to treat anisotropic diffusion in the most general form.

3. THE CHOICE OF THE LOCAL COORDINATE SYSTEM

In the absence of symmetries, there remain two distinguished local directions that, at a given location within an arbitrary magnetic field, are related to its curvature k and torsion τ and are called the normal and the binormal direction. They can be defined with the corresponding normal and binormal unit vectors, respectively. Together with the tangential unit vector, they constitute a local orthogonal trihedron fulfilling the (k - and τ -defining) Frenet–Serret relations (e.g., Marris & Passman 1969):

$$(\vec{t} \cdot \nabla)\vec{t} = k\vec{n} \quad (12)$$

$$(\vec{t} \cdot \nabla)\vec{n} = -k\vec{t} + \tau\vec{b} \quad (13)$$

$$(\vec{t} \cdot \nabla)\vec{b} = -\tau\vec{n}. \quad (14)$$

If no other diffusion axes are preferred by any process, the Frenet–Serret System constituted by the above definition of \vec{t} , \vec{n} , and \vec{b} is the most natural choice, i.e., $\vec{u} = \vec{n}$ and $\vec{v} = \vec{b}$ in Equations (3)–(11).

The transformation of the local diffusion tensor into a global coordinate system according to these equations thus requires knowledge of the dependence of the Frenet–Serret vectors on a given (non-homogeneous) magnetic field \vec{B} . Evidently, the required relations are

$$\vec{t} = \vec{B}/|\vec{B}| \quad (15)$$

$$\vec{n} = (\vec{t} \cdot \nabla)\vec{t}/k \quad (16)$$

$$\vec{b} = \vec{t} \times \vec{n}. \quad (17)$$

This trihedron can, of course, only be established for a spatially non-homogeneous field, but this (weak) condition is fulfilled in most cases of interest. If there would exist a region where the field is homogeneous, the choice of the vectors \vec{n} and \vec{b} is arbitrary (signifying isotropic perpendicular diffusion) unless no other preferential directions unrelated to the field geometry can be specified. Other principal directions unrelated to the large-scale geometry of the field could, for example, arise from non-axisymmetric turbulence. The above Equations (3)–(11) remain unaffected, however. One only needs to specify the appropriate vectors \vec{t} , \vec{n} , and \vec{v} for the respective local coordinate system.

In the following, we illustrate the procedure with the example of the well-studied HMF. We quantitatively compare the new tensor with the “traditional” one, which is only valid for isotropic perpendicular diffusion. This comparison reveals that a study of fully anisotropic turbulent diffusion within more complicated fields—like the much-discussed heliospheric Fisk field (Burger et al. 2008; Sternal et al. 2011; Fisk 1996; Burger & Hitge 2004) or complex galactic magnetic fields (Ruzmaikin et al. 1988; Beck et al. 1996)—has to be performed with even more caution than thought before.

4. AN EXAMPLE FOR THE NEW DIFFUSION TENSOR

4.1. The Heliospheric Magnetic Field

An analytical representation of the HMF, which is referred to as the *hybrid Fisk field*, can be found in Sternal et al. (2011). For a constant solar wind speed ($u_{\text{sw}} = 400 \text{ km s}^{-1}$) the HMF is

represented, using spherical polar coordinates, by the following formulation:

$$B_r = A B_e \left(\frac{r_e}{r}\right)^2, \quad (18)$$

$$B_\vartheta = B_r \frac{r}{u_{\text{sw}}} \omega^* \sin \beta^* \sin \varphi^* \quad (19)$$

$$B_\varphi = B_r \frac{r}{u_{\text{sw}}} \left[\sin \vartheta (\omega^* \cos \beta^* - \Omega_\odot) + \frac{d}{d\vartheta} (\omega^* \sin \beta^* \sin \vartheta) \cos \varphi^* \right] \quad (20)$$

with

$$\beta^*(\vartheta) = \beta F_s(\vartheta)$$

$$\omega^*(\vartheta) = \omega F_s(\vartheta)$$

$$\varphi^* = \varphi + \frac{\Omega_\odot}{u_{\text{sw}}} (r - r_\odot)$$

where

$$F_s(\vartheta) = \begin{cases} [\tanh(\delta_p \vartheta) + \tanh(\delta_p(\vartheta - \pi))] \\ -\tanh(\delta_e(\vartheta - \vartheta_b))]^2 & 0 \leq \vartheta < \vartheta_b \\ 0 & \vartheta_b \leq \vartheta \leq \pi - \vartheta_b \\ [\tanh(\delta_p \vartheta) + \tanh(\delta_p(\vartheta - \pi))] \\ -\tanh(\delta_e(\vartheta - \pi + \vartheta_b))]^2 & \pi - \vartheta_b < \vartheta \leq \pi \end{cases} \quad (21)$$

is the transition function introduced by Burger et al. (2008). In the case $F_s = 0$, the HMF reduces to the standard Parker spiral magnetic field. For a quantitative comparison of different HMF configurations, see Scherer et al. (2010).

In Equation (18), B_e denotes the magnetic field strength at $r_e = 1 \text{ AU}$, r_\odot is the solar radius, and $\Omega_\odot = 2.9 \times 10^{-6} \text{ Hz}$ is the averaged solar rotation frequency. The constant $A = \pm 1$ in Equation (18) indicates the different field directions in the northern and southern hemisphere. The values for the angle between the rotational and the so-called virtual axes of the Sun $\beta = 12^\circ$ and the differential rotation rate $\omega = \Omega_\odot/4$ are taken from Sternal et al. (2011). The parameters $\delta_p = 5$ and $\delta_e = 5$ determine the respective contributions of the Fisk and Parker fields above the poles and in the ecliptic while $\vartheta_b = 80^\circ$ is the cutoff colatitude for the Fisk-field influence. In the following, we consider two cases, a pure Parker field (i.e., setting $F_s = 0$ in Equations (19) and (20)) and the hybrid Fisk field with F_s from Equation (21). Both fields are illustrated by exemplary field lines in Figure 2.

4.2. The Local Diffusion Tensor Elements

The elements of the local diffusion tensor are chosen following the approach in Reinecke et al. (1993), i.e., as

$$\kappa_{\parallel} = \kappa_{\parallel 0} \beta \left(\frac{p}{p_0}\right) \left(\frac{B_e}{B}\right)^{a_{\parallel}} \quad (22)$$

$$\kappa_{\perp 1} = \kappa_{\perp 0} \beta \left(\frac{p}{p_0}\right) \left(\frac{B_e}{B}\right)^{a_{\perp}} \quad (23)$$

$$\kappa_{\perp 2} = \xi \kappa_{\perp 1}, \quad (24)$$

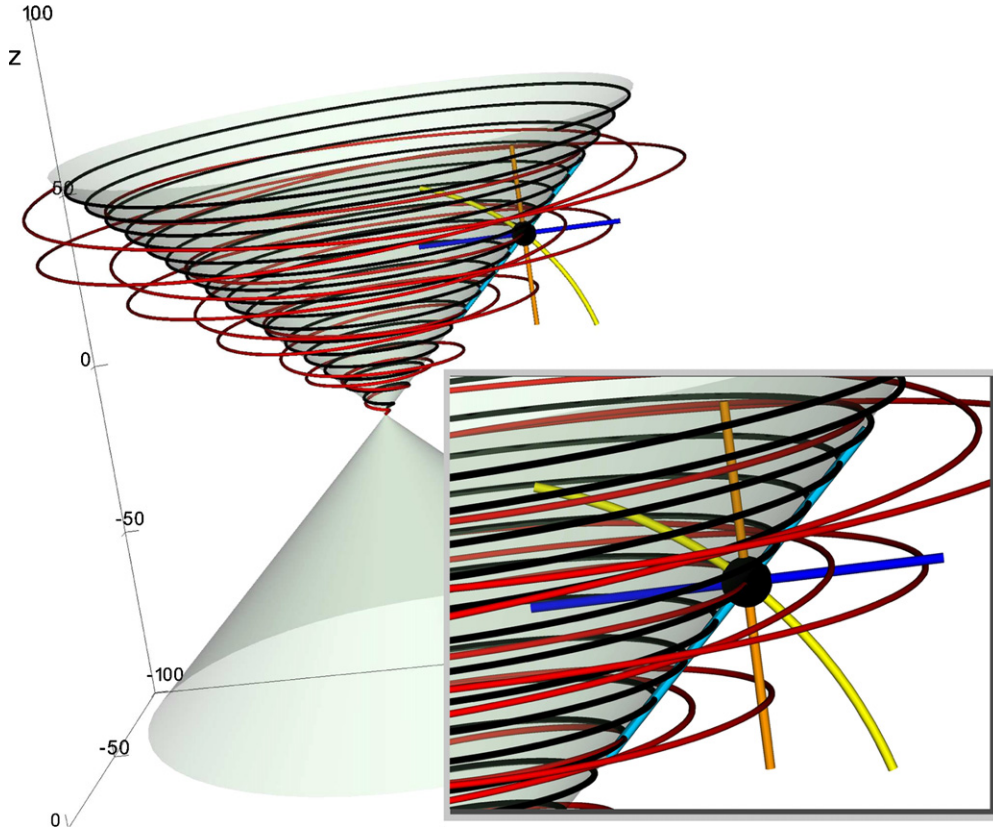


Figure 2. Hybrid Fisk and Parker fields illustrated by red and black field lines, respectively. The two local trihedrons for the Parker field are indicated with the orange and blue (Frenet–Serret) as well as the yellow and light blue (traditional) lines. Note that the traditional trihedron is always aligned to the Parker spiral cone of constant ϑ , while for the Frenet–Serret trihedron one axis (the $\kappa_{\perp 2}$ -binormal axis, orange) is nearly parallel to the z -direction. In the ecliptic, both coordinate systems coincide by definition. All distances are in units of AU.

(A color version of this figure is available in the online journal.)

where $\beta = v/c$ is the particle speed normalized to the speed of light, p is the particle momentum with the normalization constant $p_0 = 1 \text{ GeV}/c$ and B is the magnitude of the magnetic field. The scaling exponents have the values $a_{\parallel} = 0.75$ and $a_{\perp} = 0.97$. The parallel diffusion constant is $\kappa_{\parallel 0} = 0.9 \times 10^{22} \text{ cm}^2 \text{ s}^{-1}$ while $\kappa_{\perp 0} = 0.1\kappa_{\parallel 0}$. The anisotropy in perpendicular diffusion is assumed to be solely determined by the factor ξ , which is set to 2 for the following discussion. This is still a moderate choice compared with the findings of, e.g., Potgieter et al. (1997).

Although these empirical formulae for the local diffusion coefficients are not directly related to the turbulence evolution in the heliosphere and more sophisticated theoretical models for the corresponding mean free paths in parallel and perpendicular direction exist, they are still a good approximation as can be seen in the following. The result from quasilinear theory (QLT) for the mean free path (see, e.g., Shalchi 2009) is given by

$$\lambda_{\parallel}^{(\text{QLT})} = \frac{3l_{\text{slab}}}{16\pi C(\nu)} \left(\frac{B}{\delta B_{\text{slab}}} \right)^2 R^{2-2\nu} \left[\frac{2}{(1-\nu)(2-\nu)} + R^{2\nu} \right] \quad (25)$$

with

$$C(\nu) = \frac{1}{2\sqrt{\pi}} \frac{\Gamma(\nu)}{\Gamma(\nu - 1/2)} \quad (26)$$

where $\Gamma(x)$ is the gamma function, $2\nu = 5/3$ is the inertial range spectral index, $R = R_L/l_{\text{slab}}$ is the dimensionless rigidity, and $R_L = pc/(|q|B)$ is the particle Larmor radius. If one scales the bendover scale of slab turbulence as $l_{\text{slab}} = 0.03 \rho^{0.5}$ (where

ρ is the heliocentric distance in AU) and the slab turbulence variance as $\delta B_{\text{slab}}^2 = B_e^2 \rho^{-2.15}$, the radial dependence of the local tensor elements matches well with the approximative Equations (22)–(24) as shown in Figure 3. It is interesting to note that these scalings are similar to the assumptions made in Burger et al. (2008). They use the same radial dependence for l_{slab} (their exponent of $1/l_{\text{slab}} = k_{\text{min}} = 32 \rho^{0.5}$ is a typing error, private communication with the authors) and an exponent of -2.5 for the slab turbulence variance δB_{slab}^2 , which is slightly larger. Similar arguments can be made for the perpendicular diffusion. Employing for the perpendicular diffusion coefficient the result of the nonlinear guiding center (NLGC) theory of Matthaeus et al. (2003) and Shalchi et al. (2004), namely

$$\kappa_{\perp}^{(\text{NLGC})} = \left[a^2 \nu \frac{\nu - 1}{2\sqrt{3}\nu} \sqrt{\pi} \frac{\Gamma(\nu/2 + 1)}{\Gamma(\nu/2 + 1/2)} l_{2D} \frac{\delta B_{2D}^2}{B^2} \right]^{2/3} \kappa_{\parallel}^{1/3} \quad (27)$$

(see formula (15) in Burger et al. 2008) with the constant $a = 1/\sqrt{3}$. Scaling again the two-dimensional turbulence correlation length l_{2D} with $\rho^{0.5}$ and the turbulence variance δB_{2D}^2 even more weakly with $\rho^{-1.2}$ yields results similar to those obtained by Reinecke et al. (1993) for the perpendicular diffusion, as shown in Figure 3 as well.

Given the uncertainties both in the actual magnetic turbulence evolution in the heliosphere with radial distance and latitude (see, e.g., Oughton et al. 2011 for a study in which they find a much more complicated radial dependence of the slab variance)

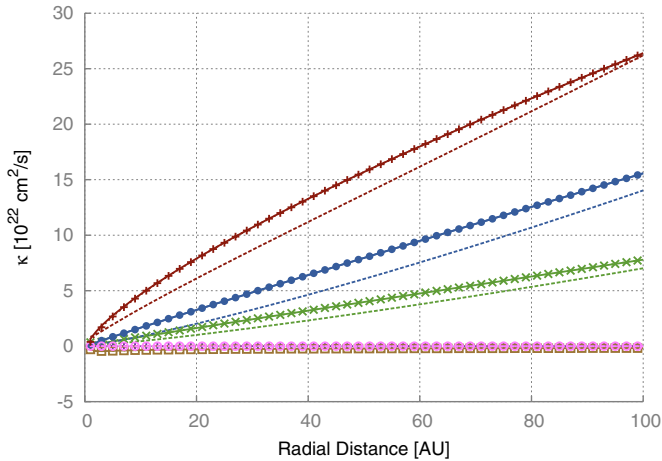


Figure 3. Dependence of the local and global tensor elements on heliocentric distance in the ecliptic plane for the Parker field. The local elements from the formulae of Equations (22)–(24) are shown as solid red (κ_{\parallel}), green ($\kappa_{\perp 1}$), and blue ($\kappa_{\perp 2}$) curves. The results for the parallel diffusion coefficient $\kappa_{\parallel}^{(QLT)} = 1/3v\lambda_{\parallel}^{(QLT)}$ (Equation (25)) and the perpendicular coefficient from $\kappa_{\perp}^{(NLGC)}$ (Equation (27)) are drawn as dashed red and green lines, respectively, while the dashed blue curve is just scaled as $\xi\kappa_{\perp}^{(NLGC)}$ with $\xi = 2$. The overlaid, color-matched symbols show the nearly perfect alignment of the κ_{rr} (green, \times), $\kappa_{\vartheta\vartheta}$ (blue, \bullet), and $\kappa_{\varphi\varphi}$ (red, $+$) global diagonal tensor elements in the ecliptic, due to the Parker field structure. All other tensor elements are almost indistinguishable from zero, as indicated by the remaining symbols.

(A color version of this figure is available in the online journal.)

and their actual relation to perpendicular or even anisotropic perpendicular diffusion in connection with three-dimensional turbulence (Shalchi 2010; Shalchi et al. 2010), we stick, in the following, with the empirical formulae of Equations (22)–(24) for this principal study.

4.3. The Structure of the Global Diffusion Tensor

Employing the formalism described in Section 3 to calculate the global diffusion tensor $\hat{\kappa}$ results in tensor elements κ_{ij} that are different from those “traditionally” used, labeled κ_{ij}^B here, with $i, j \in \{r, \vartheta, \varphi\}$. The latter are derived following the transformation presented by Burger et al. (2008), which for the Parker field is equivalent to the assumption that the local system can always be defined by $\vec{t}, \vec{n} = \vec{e}_{\vartheta} \times \vec{t}$, and $\vec{b} = \vec{e}_{\vartheta}$ (see Appendix A for the detailed transformation formulae). Both local systems are illustrated in Figure 2.

The different behavior of the tensor elements κ_{ij} and κ_{ij}^B with latitude at a heliocentric distance of 5 AU and longitude $\varphi = \pi/4$ is displayed in Figure 4 for the Parker and hybrid Fisk fields, respectively. By definition, both formulations yield the same tensor elements in the ecliptic plane, i.e., for $\vartheta = \pi/2$, while for higher latitudes the differences become more and more pronounced.

In the Parker case, e.g., the upper two rows in Figure 4, the elements κ_{rr} , $\kappa_{r\varphi}$, and $\kappa_{\varphi\varphi}$ show roughly the same behavior for all latitudes. The strongest mixing of the local elements $\kappa_{\perp 1}$ and $\kappa_{\perp 2}$ occurs in $\kappa_{\vartheta\vartheta}$, so that the deviations for high latitudes are more pronounced. The main difference appears in the off-diagonal elements $\kappa_{r\vartheta}$ and $\kappa_{\vartheta\varphi}$, which are different from zero in the general case discussed here, while they are equal to zero in the traditional approach.

The differences between the hybrid Fisk field tensor elements (shown in the lower two rows in Figure 4) are similar to those

of the Parker field described above, although they show a more complicated ϑ dependence. Note that in the traditional formulation the off-diagonal elements $\kappa_{r\vartheta}$ and $\kappa_{\vartheta\varphi}$ are already nonzero for the hybrid Fisk field and become larger in the new formulation.

The choice of longitude is arbitrary for the Parker field, since it has no φ dependence. The Fisk field, however, has significant longitudinal variations, therefore, we show the ratios of the traditional and the new tensor elements for the hybrid Fisk field with longitude (Figure 5). It can be seen that for large heliocentric distances, the deviations between both formulations vary strongly, illustrated here for a heliocentric distance of $r = 50$ AU and a heliographic colatitude of $\vartheta = \pi/4$.

We emphasize again that in the case of isotropic perpendicular diffusion ($\xi = 1$), the traditional and the new formulations are identical for any given magnetic field with non-vanishing curvature. The differences between them scale with the perpendicular anisotropy ξ (see Equation (24)).

5. APPLICATION TO THE MODULATION OF COSMIC-RAY SPECTRA

To assess the impact of the new tensor formulation on CR modulation, we employ a CR proton transport model by solving the Parker equation (Parker 1965)

$$\frac{\partial f}{\partial t} = \nabla \cdot (\hat{\kappa} \nabla f) - \vec{u}_s \cdot \nabla f + \frac{p}{3} (\nabla \cdot \vec{u}_s) \frac{\partial f}{\partial p} \quad (28)$$

to determine the differential CR intensity $j(\vec{r}, p, t) = p^2 f(\vec{r}, p, t)$ (with \vec{r} as the position in three-dimensional configuration space and p as momentum). The solar wind velocity \vec{u}_s is radially pointing outward with a constant speed of 400 km s^{-1} and $\hat{\kappa}$ is the diffusion tensor in the global frame for the Parker spiral magnetic field. This implies the Frenet–Serret trihedron of the form explicitly given in Appendix B.

The solution is obtained via a numerical integration of an equivalent system of stochastic differential equations (SDEs; Kopp et al. 2012; Gardiner 1994)

$$dx_i = A_i(x_i) dt + \sum_j B_{ij}(x_i) dW_j \quad (29)$$

for an ensemble of pseudo-particles (phase space elements) with $\hat{\kappa} = \hat{B}\hat{B}^T$ and $d\vec{W}(t) = \sqrt{dt}\vec{N}(t)$ where $\vec{N}(t)$ is a vector of normal distributed random numbers and x_i denotes the phase space coordinates. The stochastic motion $d\vec{W}(t)$ is often referred to as the Wiener process. The deterministic processes from Equation (28) such as the advection with the solar wind flow and the adiabatic energy changes are contained in the generalized velocity \vec{A} . We employ the time-backward Markov stochastic method, meaning that we trace back the pseudo-particles from a given phase space point of interest, until they hit the integration boundary. The solution to the transport equation (28) is then constructed as a proper average over the pseudo-particle orbits. For details on the general method and the numerical scheme, especially in the case of a general diffusion tensor, see Kopp et al. (2012), Strauss et al. (2011a, 2011b).

The local interstellar spectrum (LIS) of protons j_{LIS} is assumed at a heliocentric distance of $r = 100$ AU as a spherically symmetric Dirichlet boundary condition. At the inner boundary of one solar radius $r = R_{\odot}$ the pseudo-particles

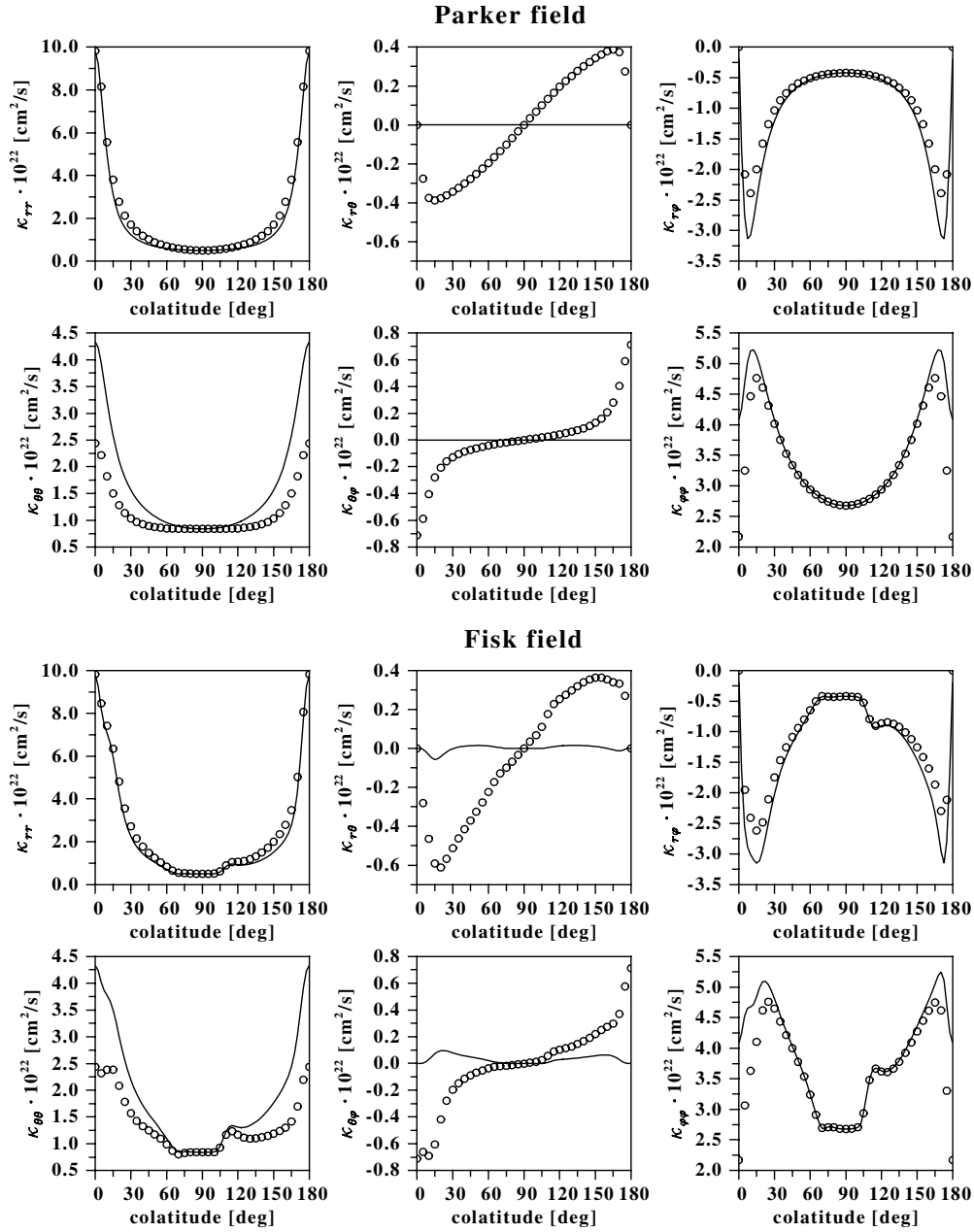


Figure 4. The complete set of six independent tensor elements κ_{ij}^B for the “traditional” tensor formulation following Burger et al. (2008; solid line) and the new κ_{ij} using the Frenet–Serret trihedron (open circles) for a fixed radius of $r = 5$ AU, a longitude of $\varphi = \pi/4$ and for varying colatitude. The upper two rows show those for the Parker field while the lower two rows show those for the hybrid Fisk field.

are reflected, which is equivalent to a vanishing gradient in the CR density there. A standard representation of the proton LIS is given by

$$j_{\text{LIS}} = 12.14 \beta (E_{\text{kin}} + 0.5 E_0)^{-2.6} \quad (30)$$

and was taken from Reinecke et al. (1993). The proton rest energy E_0 is equal to 0.938 and E_{kin} denotes the kinetic energy of a particle (both in units of GeV).

The LIS and the resulting modulated spectra are shown in Figure 6 for both tensor formulations and for several heliocentric distances. The spectra for the new Frenet–Serret tensor are

higher by up to 60% at low energies for all heliocentric distances. This is due to the enhanced diffusive flux from the modulation boundary via an effective inward diffusion along the polar axis. In the tensor formulation provided by Burger et al. (2008) this diffusion (determined by κ_{12}) cannot transport particles from the boundary into the inner heliosphere, it merely distributes the particles on a shell of fixed heliocentric distance. In the new tensor formulation exists thus a form of “pseudo-drift” produced by the off-diagonal tensor elements in the global frame, which were different or even equal to zero in the traditional formulation. This reduced modulation effect is relevant for higher energies at lower heliocentric distances, since the particles have more time to adiabatically cool (see the right panel of Figure 6).

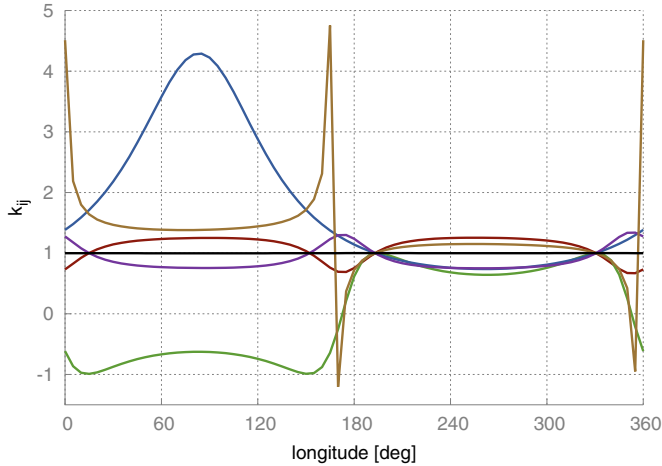


Figure 5. Ratios of the tensor elements $k_{ij} = \kappa_{ij}^B / \kappa_{ij}$ for the hybrid Fisk field plotted against heliographic longitude for a fixed heliocentric distance of $r = 50$ AU and a heliographic colatitude of $\vartheta = \pi/4$. The elements shown are k_{rr} (red), $k_{r\vartheta}$ (green), $k_{r\varphi}$ (blue), $k_{\vartheta\vartheta}$ (violet), $k_{\vartheta\varphi}$ (brown), and $k_{\varphi\varphi}$ (black). (A color version of this figure is available in the online journal.)

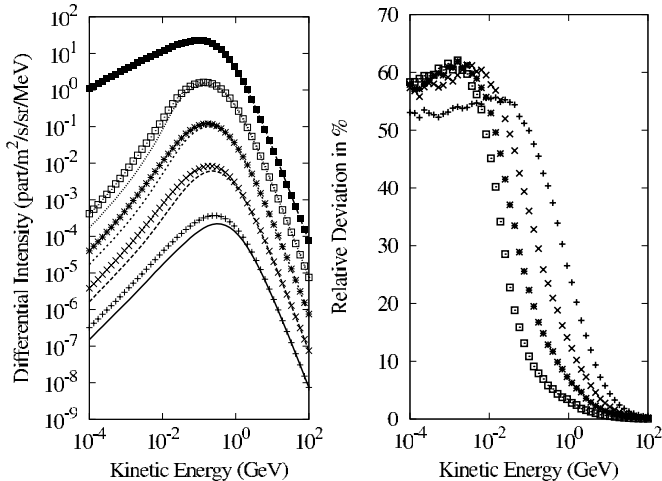


Figure 6. Modulated spectra for fully anisotropic diffusion of galactic protons for both tensor formulations. The left panel shows the resulting spectra for four heliospheric distances (1 AU, 25 AU, 50 AU, 75 AU, from bottom to top) and the LIS modulation boundary at 100 AU (solid squares). The spectra, shifted in the plot by powers of 10 for clarity (note the resulting high energy offsets), converge to the LIS for high energies. While the symbols indicate the results from the new tensor formulation with the Frenet–Serret orientation, the lines are results from an analogous computation employing the “traditional” two-angle transformation. In both cases is $\kappa_{\perp 2} = 2\kappa_{\perp 1}$. The right panel gives the relative deviations (normalized to the new results) of corresponding spectra from each other. The symbols are the same as in the left panel.

6. CONCLUSIONS

We have derived, in a global reference frame, the general form of the diffusion tensor of energetic particles in arbitrary magnetic fields. This new formulation particularly includes the case of anisotropic perpendicular diffusion that arises from field line wandering or scattering due to turbulence and requires a determination of both principal (orthogonal) perpendicular diffusion directions. Unless the turbulence is non-axisymmetric, which appears to be unlikely for the solar wind, the natural choice for these principal directions is the Frenet–Serret trihedron associated with the curvature and torsion of the magnetic field lines.

After the derivation of the formulae for all tensor elements in dependence of the Frenet–Serret unit vectors, we have first quantitatively compared the results to those published previously for the example of the heliospheric magnetic field. For the latter we have discussed two well-established alternatives, namely the Parker field and the hybrid Fisk field. While the old and new tensor formulations coincide for the case of isotropic perpendicular diffusion, the more general case of anisotropic perpendicular diffusion cannot be treated consistently with the earlier approaches. This is manifest in significant differences of corresponding tensor elements including additional non-vanishing ones.

Second, we have demonstrated the consequences of the new tensor formulation in application to the modulation of galactic CR proton spectra in the Parker heliospheric magnetic field. Solving the CR transport equation with the method of stochastic differential equations allowed us to quantify the differences between the spectra resulting from both tensor formulations for the case of perpendicular diffusion with an anisotropy of $\xi = 2$. We found those differences to amount up to 60% at energies below a few hundred MeV. Given that we used for this first principal assessment an anisotropy that is moderate as compared with findings from detailed transport and modulation studies, the fluxes can be influenced even more strongly and at even higher energies.

Besides the fact that the above results indicate the necessity to study the case of fully anisotropic diffusion in more detail within the framework of more sophisticated models of heliospheric CR modulation, they can furthermore be expected to be of importance for the particle transport in complex galactic magnetic fields for which usually isotropic (scalar) diffusion has been considered so far.

The work was carried out within the framework of the “Galactocausts” project (FI 706/9-1) funded by the Deutsche Forschungsgemeinschaft (DFG) and benefitted from the DFG-Forschergruppe FOR 1048 (project FI 706/8-1/2), the “Heliocausts” DFG-project (FI 706/6-3) as well as from the project SUA08/011 financed by the Bundesministerium für Forschung und Bildung (BMBF). We thank I. Büsching and A. Kopp for providing the basis for the SDE numerical solver. We also thank N. E. Engelbrecht for helpful discussions and an anonymous referee for a constructive evaluation.

APPENDIX A

BURGER TRANSFORMATION FORMULAE

The transformation formulae for the diffusion tensor given in Burger et al. (2008) read

$$\begin{aligned}
 \kappa_{rr}^B &= \kappa_{\perp 2} \sin^2 \zeta + \cos^2 \zeta (\kappa_{\parallel} \cos^2 \Psi + \kappa_{\perp 1} \sin^2 \Psi) \\
 \kappa_{r\vartheta}^B &= \sin \zeta \cos \zeta (\kappa_{\parallel} \cos^2 \Psi + \kappa_{\perp 1} \sin^2 \Psi - \kappa_{\perp 2}) \\
 \kappa_{r\varphi}^B &= -\sin \Psi \cos \Psi \cos \zeta (\kappa_{\parallel} - \kappa_{\perp 1}) \\
 \kappa_{\vartheta\vartheta}^B &= \kappa_{\perp 2} \cos^2 \zeta + \sin^2 \zeta (\kappa_{\parallel} \cos^2 \Psi + \kappa_{\perp 1} \sin^2 \Psi) \\
 \kappa_{\vartheta\varphi}^B &= -\sin \Psi \cos \Psi \sin \zeta (\kappa_{\parallel} - \kappa_{\perp 1}) \\
 \kappa_{\varphi\varphi}^B &= \kappa_{\parallel} \sin^2 \Psi + \kappa_{\perp 1} \cos^2 \Psi
 \end{aligned} \tag{A1}$$

with $\tan \Psi = -B_{\varphi} / \sqrt{B_r^2 + B_{\vartheta}^2}$ and $\tan \zeta = B_{\vartheta} / B_r$. Note that Kobylinski (2001) and Alania (2002) state a different formula for Ψ , namely $\tan \Psi = -B_{\varphi} / B_r$. Moreover, these formulae

involve only two angles in contrast to the general case described with the matrix A in Equation (1) in Section 2. As discussed in the text, these formulae in the given form can only hold for $\kappa_{\perp 1} \neq \kappa_{\perp 2}$ in case of special magnetic fields with $B_{\vartheta} = 0$ like that introduced by Parker.

APPENDIX B

THE PARKER FRENET–SERRET TRIHEDRON

Here, we derive the analytic expressions for the Frenet–Serret trihedron for the Parker case of the HMF. Reducing Equations (18)–(20) to the Parker field by setting $F_s = 0$ we obtain

$$\vec{t} = \frac{\vec{e}_r - \tan \chi \vec{e}_{\varphi}}{\sqrt{1 + \tan^2 \chi}} \quad (\text{B1})$$

for the tangential vector, with $\tan \chi = \omega/u_s r \sin \vartheta$. The easiest way to derive the normal vector \vec{n} is to calculate $(\vec{t} \cdot \nabla)\vec{t} = k\vec{n}$ (where k is the curvature, see Equation (12)) and to normalize appropriately. After some straightforward calculation, one arrives at

$$\vec{n} = -\frac{E(\tan \chi \vec{e}_r + \vec{e}_{\varphi}) + F\vec{e}_{\vartheta}}{\sqrt{E^2(\tan^2 \chi + 1) + F^2}} \quad (\text{B2})$$

where the abbreviations

$$E = \frac{\tan^2 \chi}{r} + \frac{\omega}{u_s} \frac{\sin \vartheta}{1 + \tan^2 \chi}, \quad F = \frac{\tan^2 \chi \cos \vartheta}{r \sin \vartheta} \quad (\text{B3})$$

have been introduced. The binormal vector is now simply the cross product $\vec{b} = \vec{t} \times \vec{n}$, which yields

$$\vec{b} = \frac{-F(\tan \chi \vec{e}_r + \vec{e}_{\varphi}) + E(\tan^2 \chi + 1)\vec{e}_{\vartheta}}{\sqrt{F^2(\tan^2 \chi + 1) + E^2(\tan^2 \chi + 1)^2}}. \quad (\text{B4})$$

Equations (B1), (B2), and (B4) are the explicit formulae for the Frenet–Serret trihedron in the case of the heliospheric Parker field. Corresponding but much longer expressions can, in principle, be obtained for the Fisk field as well.

REFERENCES

- Alania, M. V. 2002, *Acta Phys. Pol. B*, **33**, 1149
 Beck, R., Brandenburg, A., Moss, D., Shukurov, A., & Sokoloff, D. 1996, *ARA&A*, **34**, 155
 Belcher, J. W., & Davis, L., Jr. 1971, *J. Geophys. Res.*, **76**, 3534
 Burger, R. A., & Hitge, M. 2004, *ApJ*, **617**, L73
 Burger, R. A., Krüger, T. P. J., Hitge, M., & Engelbrecht, N. E. 2008, *ApJ*, **674**, 511
 Burger, R. A., Potgieter, M. S., & Heber, B. 2000, *J. Geophys. Res.*, **105**, 27447
 Ferreira, S. E. S., Potgieter, M. S., Burger, R. A., Heber, B., & Fichtner, H. 2001, *J. Geophys. Res.*, **106**, 24979
 Fisk, L. A. 1996, *J. Geophys. Res.*, **101**, 15547
 Gardiner, C. W. 1994, *Stochastic Methods* (Berlin: Springer)
 Horbury, T. S., Balogh, A., Forsyth, R. J., & Smith, E. J. 1995, *Geophys. Res. Lett.*, **22**, 3405
 Jokipii, J. R. 1973, *ApJ*, **182**, 585
 Jokipii, J. R. 2001, *J. Geophys. Res.*, **106**, 15841
 Jokipii, J. R., Kóta, J., Giacalone, J., Horbury, T. S., & Smith, E. J. 1995, *Geophys. Res. Lett.*, **22**, 3385
 Kelly, J., Dalla, S., & Laitinen, T. 2012, *ApJ*, in press (arXiv:1202.6237)
 Kobylinski, Z. 2001, *Adv. Space Res.*, **27**, 541
 Kopp, A., Buesching, I., Strauss, R., & Potgieter, M. 2012, *CoPhC*, **183**, 530
 Lionello, R., Linker, J. A., Mikić, Z., & Riley, P. 2006, *ApJ*, **642**, L69
 Marris, A. W., & Passman, S. L. 1969, *Arch. Ration. Mech. Anal.*, **32**, 29
 Matthaeus, W. H., Qin, G., Bieber, J. W., & Zank, G. P. 2003, *ApJ*, **590**, L53
 Oughton, S., Matthaeus, W. H., Smith, C. W., Breech, B., & Isenberg, P. A. 2011, *J. Geophys. Res.*, **116**, 8105
 Parker, E. 1965, *Planet. Space Sci.*, **13**, 9
 Parker, E. N. 1958, *ApJ*, **128**, 664
 Potgieter, M. S., Haasbroek, L. J., Ferrando, P., & Heber, B. 1997, *Adv. Space Res.*, **19**, 917
 Reinecke, J. P. L., Moraal, H., & McDonald, F. B. 1993, *J. Geophys. Res.*, **98**, 9417
 Ruffolo, D., Chuychai, P., Wongpan, P., et al. 2008, *ApJ*, **686**, 1231
 Ruzmaikin, A. A., Shukurov, A. M., & Sokolov, D. D. (ed.) 1988, *Magnetic Fields of Galaxies* (Dordrecht: Kluwer)
 Scherer, K., Fichtner, H., Effenberger, F., Burger, R. A., & Wiengarten, T. 2010, *A&A*, **521**, A1
 Schlickeiser, R. 2002, *Cosmic Ray Astrophysics* (Berlin: Springer)
 Shalchi, A. (ed.) 2009, *Nonlinear Cosmic Ray Diffusion Theories* (Berlin: Springer)
 Shalchi, A. 2010, *ApJ*, **720**, L127
 Shalchi, A., Bieber, J. W., & Matthaeus, W. H. 2004, *ApJ*, **604**, 675
 Shalchi, A., Li, G., & Zank, G. P. 2010, *Ap&SS*, **325**, 99
 Sternal, O., Engelbrecht, N. E., Burger, R. A., et al. 2011, *ApJ*, **741**, 23
 Strauss, R. D., Potgieter, M. S., Büsching, I., & Kopp, A. 2011a, *ApJ*, **735**, 83
 Strauss, R. D., Potgieter, M. S., Kopp, A., & Büsching, I. 2011b, *J. Geophys. Res.*, **116**, A12
 Tautz, R. C., & Shalchi, A. 2012, *ApJ*, **744**, 125
 Tautz, R. C., Shalchi, A., & Dosch, A. 2011, *J. Geophys. Res.*, **116**, 2102
 Turner, A. J., Gogoberidze, G., Chapman, S. C., Hnat, B., & Müller, W.-C. 2011, *Phys. Rev. Lett.*, **107**, 095002
 Webb, G. M., Kaghshvili, E. K., le Roux, J. A., et al. 2009, *J. Phys. A: Math. Gen.*, **42**, 235502
 Weinhorst, B., Shalchi, A., & Fichtner, H. 2008, *ApJ*, **677**, 671
 Wicks, R. T., Forman, M. A., Horbury, T. S., & Oughton, S. 2012, *ApJ*, **746**, 103